Anisotropically and High Entanglement of Biphoton States Generated in Spontaneous Parametric Down-Conversion

M. V. Fedorov, M. A. Efremov, and P. A. Volkov
A. M. Prokhorov General Physics Institute of Russian Academy of Sciences, 117942, Moscow, Russia

E. V. Moreva*
Moscow Engineering Physics Institute (State University), 115409, Moscow, Russia

S. S. Straupe and S. P. Kulik
Faculty of Physics, Moscow State University, 119992, Moscow, Russia
(Received 20 December 2006; published 6 August 2007)

We show both theoretically and experimentally that biphoton wave packets generated via spontaneous parametric down-conversion can be strongly anisotropic and highly entangled. The conditions under which these effects exist are found and discussed.

DOI: 10.1103/PhysRevLett.99.063901 PACS numbers: 42.65.Lm, 03.65.Ud, 03.67.Mn

Introduction.—Entanglement of biphoton states formed in spontaneous parametric down-conversion (SPDC) is a hot topic of modern quantum optics and quantum information. The most often considered kind of entanglement in this field is the entanglement with respect to the photon polarization variables. But a growing interest in entanglement with respect to continuous variables has arisen, such as photon momentum or coordinates [1–10], frequency entanglement [11,12]. Note that compared to discrete variables, entanglement in continuous variables is much more complicated, far less investigated, and many well-known features of entangled discrete-variable states do not have direct counterparts in the case of continuous variables. In this Letter we investigate both theoretically and experimentally angular (momentum) structure of SPDC biphoton coincidence and single-photon distributions, with special attention paid to a proper account of the anisotropy effects. Namely, it turns out that the biphoton coincidence angular distributions depend strongly on the crystal orientation. As far as we know, this effect has never been observed earlier experimentally or described theoretically.

Also, we evaluate the degree of entanglement for biphoton states, which is shown to be very high. To do this we apply here the recently suggested operational method [9,13], which relates the degree of entanglement to the parameter $R = \Delta k^{(s)}/\Delta k^{(c)}$. $\Delta k^{(s)}$ and $\Delta k^{(c)}$ are the experimentally measurable single-particle and coincidence widths of the corresponding photon momentum wave packets. For nonentangled states $R = 1$, whereas any deviations from the exact equality of $\Delta k^{(s)} = \Delta k^{(c)}$ serves as an indication that the bipartite state under consideration becomes entangled. For evaluating the degree of entanglement of the 2D biphoton state as a whole, we use a measure R_{overall} given by the product of parameters $R_{\parallel}$ and $R_{\perp}$ for two orthogonal geometries.

Theoretical description.—Let us consider a collinear and degenerate type I SPDC process, when extraordinary pump photon of a frequency ω_p decays in two ordinary photons (signal and idler) with equal frequencies $\omega_p/2$ and propagating more or less along the pump beam. In 3D, refractive index surfaces for extraordinary $[n_e(\vec{r};\omega_p)]$ and ordinary $[n_o(\vec{r};\omega_p/2)]$ waves in an anisotropic crystal are, correspondingly, an ellipsoid and a sphere. Figure 1(a) shows sections of these figures by three coordinate planes (xz), (xy), and (yz). The optical axis of a crystal is taken directed along the Ox axis. The arc DB is a part of the circle by which the sphere and ellipsoid cross each other. We assume that the pump is not a single plane wave but is given by a coherent superposition of plane waves with wave vectors $\vec{k}_p$ filling a cone, the axis of which coincides with the Oz' axis, and the angular width α is finite. The detectors are assumed to be installed along some line $O'\xi$ in the plane $((x'O'y'))$. Axis $O'x'$ belongs to the plane (xz) and $O'y' \parallel Oy$. The angle χ between $O'\xi$ and $O'x'$ serves a varying parameter. The cases $\chi = 0$ $(O'\xi \parallel O'x')$ and $\chi = \pi/2$ $(O'\xi \parallel O'y')$ are referred to below as the $\parallel$ and $\perp$ geometries of measurement.

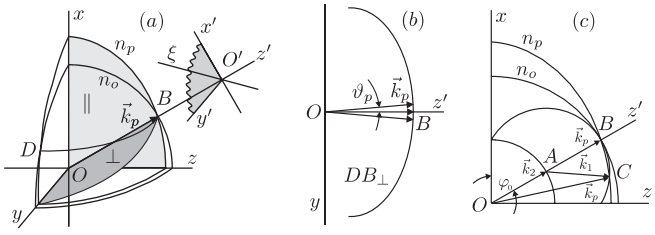

FIG. 1. (a) Octant of the refractive index surfaces $n_e(\vec{r})$ and $n_o(\vec{r})$ for pump and signal photons; (b), (c) are two perpendicular section by the planes $\perp$ and $\parallel$ shaded in (a); $O'\eta$ is the axis in the plane $(x'y')$ perpendicular to $O'\xi$.

To describe the main effects we predict in the most straightforward way, we consider here explicitly only the case when transverse ($\perp$ to Oz') components of wave vectors $\vec{k}_p$, $\vec{k}_1$, and $\vec{k}_2$ belong to the observation plane $(\xi z')$. Generalizations will be described elsewhere [14]. In the approximation of a wide crystal the condition $k_{p\xi} = k_{1\xi} + k_{2\xi}$ holds, and the momentum-representation biphoton wave function is known [4] to be given by

$$\Psi(k_{1\xi}, k_{2\xi}) \propto E_p^*(k_{1\xi} + k_{2\xi})\mathrm{sinc}\left(\frac{L(k_{pz'} - k_{1z'} - k_{2z'})}{2}\right), \tag{1}$$

where L is the crystal length in the z' direction, E_p is the momentum representation of the pump wave transverse profile, and longitudinal components of the photon wave vectors are expressed via transverse ones as $k_{1z'} = (k_1^2 - k_{1\xi}^2)^{1/2}$, $k_{2z'} = (k_2^2 - k_{2\xi}^2)^{1/2}$, and $k_{pz'} = (k_p^2 - k_{p\xi}^2)^{1/2}$.

In the near-axis approximation the square roots determining $k_{1,2,pz'}$ can be expanded in powers of $k_{1,2\xi}$ with only zero- and second-order terms to be retained. The zero-order term $k_p - k_1 - k_2$ is usually dropped [5,7,9,10]. Our key observation is that this can be done only in the $\perp$ geometry ($\chi = \pi/2$), when the pump wave vector $\vec{k}_p$ has the same length for all its directions in the (z', ξ) plane [see Fig. 1(b)]. At all other values of the angle χ the detuning $k_p - k_1 - k_2$ cannot be taken identically equal zero because the term k_p itself depends on the orientation of the vector $\vec{k}_p$. A typical picture showing an orientation-dependent length of the pump wave vector is shown in Fig. 1(c) for the $\parallel$ geometry ($\chi = 0$).

Though formally looking as zero order in $k_{1,2\xi}$, the detuning $k_p - k_1 - k_2$ can be expressed via transverse components of the wave vectors of emitted photons and it appears, actually, to be linear in $k_{1,2\xi}$. This connection follows directly from the geometry of Fig. 1(c). Not dwelling here on further details of the derivation (see Ref. [15]), let us reproduce only the final result of transforming Eq. (1) and expressing it in terms of scattering angles outside of the crystal $\theta_{1,2} = 2k_{1,2\xi}c/k_p^{(0)}$

$$\Psi(\theta_1, \theta_2) \propto \tilde{E}_p^*\left(\frac{\theta_1 + \theta_2}{2}\right)\mathrm{sinc}\left\{\frac{Lk_p^{(0)}}{16n_o}[4n_p' \cos\chi(\theta_1 + \theta_2) + (\theta_1 - \theta_2)^2]\right\}. \tag{2}$$

Here $\tilde{E}_p(\theta_p)$ is the pump amplitude angular distribution outside the crystal, $\theta_p = \frac{1}{2}(\theta_1 + \theta_2)$ is the angle between the pump wave vector outside of the crystal and the laser axis Oz', $n_p' = \partial n_p/\partial\vartheta_p|_{\vartheta_p=0}$, ϑ_p is the angle between $\vec{k}_p$ (in the crystal) and Oz' calculated in the $\parallel$ geometry, and $k_p^{(0)} = \omega_p/c$. For $LiIO_3$ crystal and $\lambda_p = 325$ nm we consider here, $n_p' = -0.1436$ and $\varphi_0 = 60.44°$ [in Fig. 1(c)].

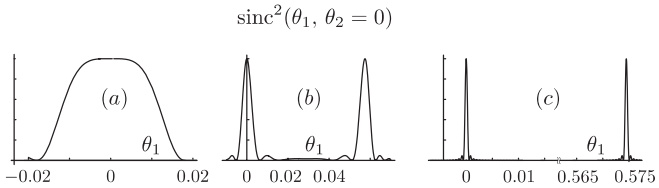

FIG. 2. The sinc^2 function of Eq. (2) at (a) $\chi = 90°$, (b) $\chi = 84°$, and (c) $\chi = 0$, θ_1 in radians; the crystal length L is taken equal to 1.5 cm.

Anisotropy.—Equation (2) differs from the traditional one [5,7,9] by the first term in the square brackets in the argument of the sinc function. The role of this term is illustrated by Fig. 2 where the squared sinc function of Eq. (2) is plotted in its dependence θ_1 at $\theta_2 = 0$ and three different values of χ. Starting from $\chi = \pi/2$ with a decreasing value of χ, the structure of the curves in Fig. 2 changes drastically. Already at very small deviations from $\chi = \pi/2$ a single wide peak splits in two peaks (the second one is due to the noncollinear phase matching), spacing between them grows, and the peaks are getting very narrow. For comparison, the width of the only peak at $\chi = \pi/2$ is 24 mrad, whereas at $\chi = 0$ it shrinks to 0.5 mrad.

Coincidence and single-particle distributions.—Coincidence distributions of photons are determined by the squared absolute values of the narrower of two function in the product of Eq. (2). In the cases of $\parallel$ and $\perp$ geometry the narrower functions are, correspondingly, sinc^2 and E_p^2. In Fig. 3 the curve describing the dependence of these functions on θ_1 at $\theta_2 = 0$ are plotted in solid lines. The pump E_p^2 in the $O'y'$ direction is taken in the form of a sinc^2 function with the divergency $\alpha = 4.1$ mrad. The half-height widths of the coincidence distributions are easily found directly from Eq. (2) to be given by:

$$\Delta\theta_1^{(c)\parallel} = \frac{2.784 \times 4n_0}{Lk_p^{(0)}|n_p'|}, \qquad \Delta\theta_1^{(c)\perp} = 2\alpha. \tag{3}$$

Numerically $\Delta\theta_1^{(c)\parallel} = 0.5$ mrad and $\Delta\theta_1^{(c)\perp} = 8.2$ mrad. Their ratio $\Delta\theta_1^{(c)\perp}/\Delta\theta_1^{(c)\parallel} = 16.4$ can be considered as a measure of anisotropy, which is seen to be quite high.

Single-particle distribution in the $\parallel$ geometry is received by a direct integration of the squared wave function (2) over θ_2. To find the single-particle distribution in the $\perp$

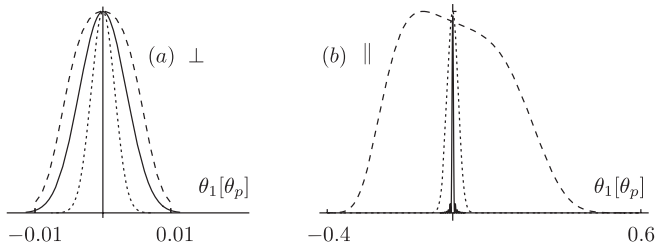

FIG. 3. Coincidence (solid lines) and single-particle (dashed lines) angular distributions for (a) $\chi = \pi/2$ and (b) $\chi = 0$; all curves are normalized by one at their maxima.

geometry we have to take into account contribution of noncollinear SPDC phase matching with $k_{2\eta} \neq 0$ [14]. In both cases, we come to rather simple formulas

$$\frac{dw_{\parallel}^{(s)}}{d\theta_1} \propto \mathrm{sinc}^2\left(\frac{2.784\theta_1^2}{2|n_p'|\alpha}\right), \qquad \frac{dw_{\perp}^{(s)}}{d\theta_1} \propto \exp\left[-\frac{\ln(2)}{\alpha_0^2}\frac{\theta_1^4}{n_p'^2}\right]. \tag{4}$$

Here the pump in the $O'x'$ direction is taken Gaussian with $\alpha_0 = 1.5$ mrad, which corresponds to the experimental conditions described below. The single-particle angular distributions in both geometries are shown in Fig. 3 by dashed lines. The asymmetry of single-particle distribution for $\parallel$ geometry appears from the factors which are not shown in Eq. (4) [14]. The half-height widths of the single-particle distributions are given by

$$\Delta\theta_1^{(s)\parallel} = 2\sqrt{|n_p'|\alpha}, \qquad \Delta\theta_1^{(s)\perp} = 2\sqrt{|n_p'|\alpha_0}, \tag{5}$$

and numerically $\Delta\theta_1^{(s)\parallel} \approx 48.53$ mrad, $\Delta\theta_1^{(s)\perp} \approx 29.35$ mrad.

Entanglement.—The wave packet widths presented in Eqs. (3) and (5) can be used to estimate the width-ratio parameters R for $\parallel$ and $\perp$ geometries

$$R_{\parallel} = \frac{Lk_p^{(0)}|n_p'|^{3/2}\sqrt{\alpha}}{5.568n_o} = 94.6, \qquad R_{\perp} = \frac{\sqrt{|n_p'|\alpha_0}}{\alpha} = 3.6. \tag{6}$$

Validity of the width-ratio parameters for evaluation of the degree of entanglement has been proven for double-Gaussian 1D bipartite wave functions [9,13]. However, the biphoton wave function is more complicated. To check validity of the R parameters as entanglement quantifiers we evaluated theoretically also the EPR entanglement parameter, for the $\parallel$ geometry defined as

$$C_{\mathrm{EPR}}^{\parallel} = \frac{4\ln(2)}{\Delta\xi_1^{(c)} \times \Delta k_{1\xi}^{(c)}}, \tag{7}$$

where $\Delta\xi_1^{(c)}$ and $\Delta k_{1\xi}^{(c)} = \frac{1}{2}k_p\Delta\theta_1^{(c)}$ are the coordinate and momentum coincidence wave packet widths. Derivation of explicit expressions for $C_{\mathrm{EPR}}^{\parallel}$ will be given elsewhere [14], but the final result appears to be identical practically to that of Eq. (6) for $R_{\parallel}$, and numerically $C_{\mathrm{EPR}}^{\parallel} \approx 96 \approx R_{\parallel}$.

At the same time one should remember that the biphoton state is two dimensional and anisotropic. This complicates both rigorous definition and measurement of the overall biphoton entanglement quantifier. Here we restrict ourselves by giving the simplest estimate of such a parameter R_{overall} as a product of $R_{\parallel}$ and $R_{\perp}$. Such a definition was shown to be correct [7] by calculating Schmidt number K [16,17] for the isotropic 2D biphoton wave function. It was modeled by the product of two double-Gaussian functions. The calculated in such a way parameter K was shown to differ only slightly from the numerically calculated one found without modeling by Gaussian functions. Any further generalizations for more realistic but complicated cases are not known up to now. In any case, by using the definition given above and Eqs. (6), we find

$$R_{\mathrm{overall}} = R_{\parallel} \times R_{\perp} = \frac{Lk_p^{(0)}n_p'^2}{5.568n_o}\sqrt{\frac{\alpha_0}{\alpha}} \approx 346. \tag{8}$$

This is a huge degree of entanglement achieved mainly owing to consideration a rather long crystal with a relatively large value of the refractive index angular derivative $|n_p'|$. Equation (8) shows that increasing the angular width of the pump α in one direction compared to another one, α_0, does not lead to further increasing degree of entanglement. At $\alpha = \alpha_0$ the overall degree of entanglement appears to be independent of the pump divergency. It is important to notice that restrictions on the pump divergency α, the crystal length L and anisotropy $|n_p'|$ follow from the validity conditions of all the derived results

$$\alpha L|n_p'| \gg \lambda_p, \tag{11}$$

which is quite well fulfilled for parameters we consider.

Note at last that an important theoretical problem, still awaiting its solution, is the calculation of the overall Schmidt number K for a complete 2D anisotropic biphoton wave function and comparison of K with R_{overall} (8).

Experimental setup.—The experimental setup is shown in Fig. 4. To generate the entangled photons we use type I and 15 mm-length lithium-iodate crystal pumped with a 5 mW cw-helium-cadmium laser operating at 325 nm with divergency 1.5 mrad. The correlated photons generated via SPDC process with equal polarization and wavelength 650 nm are separated from the pump by dichroic mirror. Interference filters centered at 650 nm with a bandwidth of 10 nm are placed in each arm of Hanbury Brown-Twiss scheme. To measure coincidence and single-photon distributions in the transverse momenta we use the lens with focal length $F = 62$ cm. Two single-photon detectors (D) are positioned in focal plane of the lens. In most cases we fix position of the first detector at the maximum of count rate and scan another one to register both distributions as a function of detector displacement. Its position (x) relates to the angular mismatch (θ) as $x = F\tan\theta$.

Results and discussion.—The main idea behind performed experiment is to check the formulas of

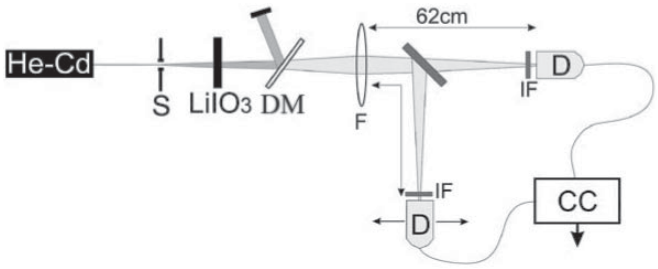

FIG. 4. Experimental setup for measuring single and coincidence probability distributions.

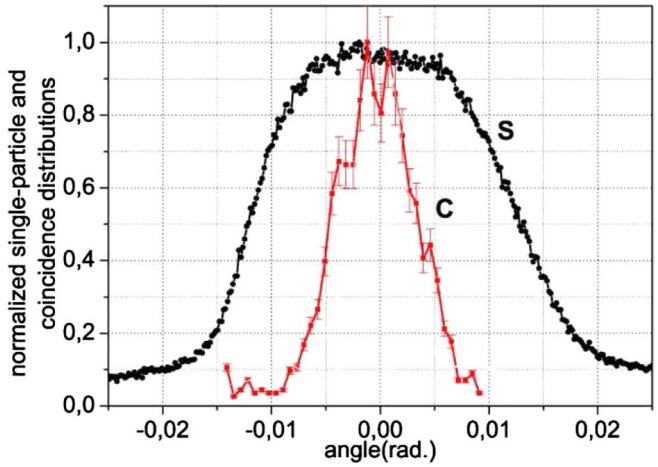

FIG. 5 (color online). Experimental results: normalized single-particle and coincidence distributions for ⊥ geometry.

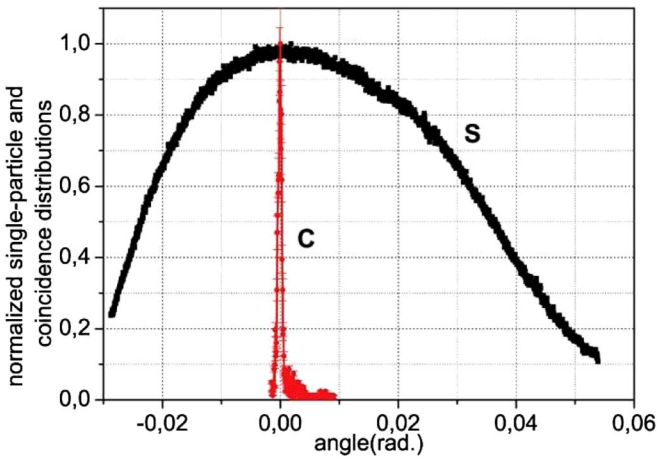

FIG. 6 (color online). Experimental results: normalized single-particle and coincidence distributions for ∥ geometry.

Eqs. (2)–(6) and, in such a way, to compare the ∥ and ⊥ geometries of Fig. 1. To see how the angular distribution of the pump effects upon biphoton angular distributions, we have artificially and anisotropically broadened the pump by installing a slit (S) in front of the crystal. The slit was installed always vertically to provide angular broadening in the horizontal direction, where the detector(s) scan, whereas the crystal optical axis could be lying either in the vertical or horizontal planes. The slit thickness was 70 mkm, which corresponds to the 4.1 mrad pump divergency in the direction perpendicular to the slit.

The pictures of Fig. 5 and 6 show two sets of angular distributions corresponding to both single-particle and coincidences measurements, which are performed for different geometries (⊥ and ∥). These plots allow one to evaluate the degree of entanglement directly from experimental data by using Eq. (8). Figure 5 corresponds to the ⊥ geometry. The width of the single-particle distribution is 25 mrad whereas the width of the coincidence one is 8.4 mrad, i.e., twice wider than the width of the pump [in accordance with the second Eq. (3)]. The ratio $\Delta k_{1\perp}^{(s)}/\Delta k_{1\perp}^{(c)} = 3$, which is close to the theoretical estimate of 3.5. The results occurring for the ∥ geometry are shown in Fig. 6. Here the widths of single and coincidence distributions are 60 mrad and 0.75 mrad, correspondingly. Their ratio is 80, which is much greater than in the previous case and very close to that predicted by theory $R_{k\parallel} = 94.6$.

The measure R_{overall} introduced above takes the value 240. Although it is distinctly less then the value estimated numerically (8) we think it caused mainly by the factors that were not considered like setup misalignment, finite spectrum of the SPDC, etc.

To conclude, we have shown both theoretically and experimentally that there is a possibility of creating highly entangled biphoton states under conditions when the pump beam has significant divergence while the nonlinear crystal is sufficiently long and its anisotropy is taken into account. $LiIO_3$ appears to be one of the best crystals satisfying to these conditions.

This work was supported in part by the Russian Foundation for Basic Research (Projects No. 05-02-16469 and No. 06-02-16769), the RF President's Grant No. MK1283.2005.2, the Leading Russian Scientific Schools (Project No. 4586.2006.2), and by the US Army International Technology Center—Atlantic, Grant No. RUE1-1616-MO-06.

*ekaterina.moreva@gmail.com

[1] A. Einstein, B. Podolsky, and N. Rosen, Phys. Rev. **47**, 777 (1935).
[2] M. H. Rubin, Phys. Rev. A **54**, 5349 (1996).
[3] A. V. Burlakov *et al.*, Phys. Rev. A **56**, 3214 (1997).
[4] C. H. Monken, P. H. Souto Ribeiro, and S. Padua, Phys. Rev. A **57**, 3123 (1998).
[5] S. P. Walborn, A. N. de Oliveira, and C. H. Monken, Phys. Rev. Lett. **90**, 143601 (2003).
[6] M. D'Angelo *et al.*, Phys. Rev. Lett. **92**, 233601 (2004).
[7] C. K. Law and J. H. Eberly, Phys. Rev. Lett. **92**, 127903 (2004).
[8] J. C. Howell *et al.*, Phys. Rev. Lett. **92**, 210403 (2004).
[9] M. V. Fedorov *et al.*, J. Phys. B **39**, S467 (2006).
[10] K. W. Chan, C. K. Law, and J. H. Eberly, Phys. Rev. A **68**, 022110 (2003).
[11] W. P. Grice and I. A. Walmsley, Phys. Rev. A **56**, 1627 (1997).
[12] Y. H. Kim and W. P. Grice, Opt. Lett. **30**, 908 (2005).
[13] M. V. Fedorov *et al.*, Phys. Rev. A **69**, 052117 (2004); **72**, 032110 (2005).
[14] M. V. Fedorov *et al.* (to be published).
[15] M. V. Fedorov *et al.*, arXiv:quant-ph/0612104.
[16] R. Grobe, K. Rzazewski, and J. H. Eberly, J. Phys. B **27**, L503 (1994).
[17] A. Ekert and P. L. Knight, Am. J. Phys. **63**, 415 (1995).